

## Geochemical and Nd-Sr-Pb isotopic composition of Mesozoic volcanic rocks in the Songliao basin, NE China

PU-JUN WANG,<sup>1</sup> FUKUN CHEN,<sup>2\*</sup> SHU-MIN CHEN,<sup>3</sup> WOLFGANG SIEBEL<sup>4</sup> and MUHARREM SATIR<sup>4</sup>

<sup>1</sup>Earth Sciences' College, Jilin University, Changchun 130061, Jilin Province, China

<sup>2</sup>Laboratory for Radiogenic Isotope Geochemistry, Institute of Geology and Geophysics, Chinese Academy of Sciences, P.O. Box 9825, Beijing 100029, China

<sup>3</sup>Daqing Institute of Exploration and Development, Daqing 163712, China

<sup>4</sup>Institute für Geowissenschaften, Universität Tübingen, Tübingen 72074, Germany

(Received November 8, 2004; Accepted September 1, 2005)

Mesozoic volcanic rocks exposed in the Songliao basin form a major part of the basin fill and are the important petroleum reservoir rocks. Petrogenesis of these volcanic rocks and their tectonic setting, however, are poorly understood due to lack of sufficient chemical and isotopic data. These volcanic rocks cover a wide compositional spectrum ranging from basaltic trachyandesite to high-silica rhyolite. They can be divided into two formations, the upper Jurassic Huoshiling formation (157–146 Ma) with dominant dark gray andesite and the lower Cretaceous Yingcheng formation (136–113 Ma) with dominant yellowish rhyolite. Compositionally, these rocks are peraluminous to metaluminous, high-K to medium-K, calc-alkaline. They are enriched in large-ion lithophile and light rare earth elements, depleted in high field strength and heavy rare earth elements, and commonly display negative anomalies of Nb, Ti and P. Initial  $^{87}\text{Sr}/^{86}\text{Sr}$  ratios and initial  $\epsilon_{\text{Nd}}$ -values of these volcanic rocks range from 0.7034 to 0.7106 and from –3.4 to 5.3, respectively, and their  $\delta^{18}\text{O}$  values vary from 3.2‰ to 14.8‰. Initial  $^{206}\text{Pb}/^{204}\text{Pb}$  and  $^{207}\text{Pb}/^{204}\text{Pb}$  ratios have ranges of 17.65 to 18.22 and 15.52 to 15.57, respectively. The characteristic in Nd and Sr isotopic composition probably indicates a mixing of enriched MORB-like material and crustal component. Primary magmas for both the Jurassic and Cretaceous volcanic rocks could be derived from metasomatized enriched MORB-like sources, but the Cretaceous rhyolites commonly show crustal assimilation indicated by high initial  $^{87}\text{Sr}/^{86}\text{Sr}$  ratios and low initial  $\epsilon_{\text{Nd}}$  values. Whether the volcanic rocks in the Songliao basin formed related either to the post-collisional setting of the Mongolia-Okhotsk suture or the subduction of the western Pacific plate remains to be discussed.

Keywords: geochemistry, Nd-Sr-Pb isotopes, Mesozoic, volcanic rock, Songliao basin

### INTRODUCTION

Sedimentary basins and mountain ranges formed in the Mesozoic produce the predominant structural relief of NE China (e.g., Cheng *et al.*, 1990), though the relationship between the mountain building and the basin formation are not well understood yet. Mesozoic volcanic and pyroclastic rocks comprise a major part of the mountains and the early basin fills. They are also the important reservoir rocks in the Songliao basin. Three hypotheses have been previously proposed for the geodynamic setting of the volcanic series in the Songliao basin. Traditionally, they are considered as products in a continental rifting environment (e.g., Liu *et al.*, 1993; Liu and Ma, 1998). Other interpretations in contrast considered them as products in an active continental setting related either to the subduction of the Pacific plate under the Eurasia

plate in Mesozoic (e.g., Zhao *et al.*, 1998; Sun *et al.*, 2000) or to the closure of the Mongolia-Okhotsk ocean between the Siberia and North China plates from 255 Ma to 94 Ma (Scotese *et al.*, 1988). The rift model is not evidenced in the volcanic rock association. They mainly show calc-alkaline signature and lack of basalts and peralkaline rocks that are considered for typical rifting environments (Harangi, 1994). However, the model related to the Pacific plate subduction can hardly explain the sharp change in sedimentary facies and tectonic system at about 113 Ma in the basin (Fig. 1), since volcanic successions are all beneath the hiatus and show significant difference in lithology, distribution and structures from the overlying sedimentary sequence of NNE-strike that is clearly controlled by the Pacific tectonic regime (e.g., Liu *et al.*, 1993). The Mongolia-Okhotsk ocean was closed within the Songliao basin section in middle Jurassic (Zhao *et al.*, 1996) prior to the volcanism of 157 Ma to 113 Ma in the basin, therefore, the syn-subduction cannot be favored for the origin of the volcanic rocks in the Songliao Basin.

\*Corresponding author (e-mail: fukun-chen@mail.igcas.ac.cn)

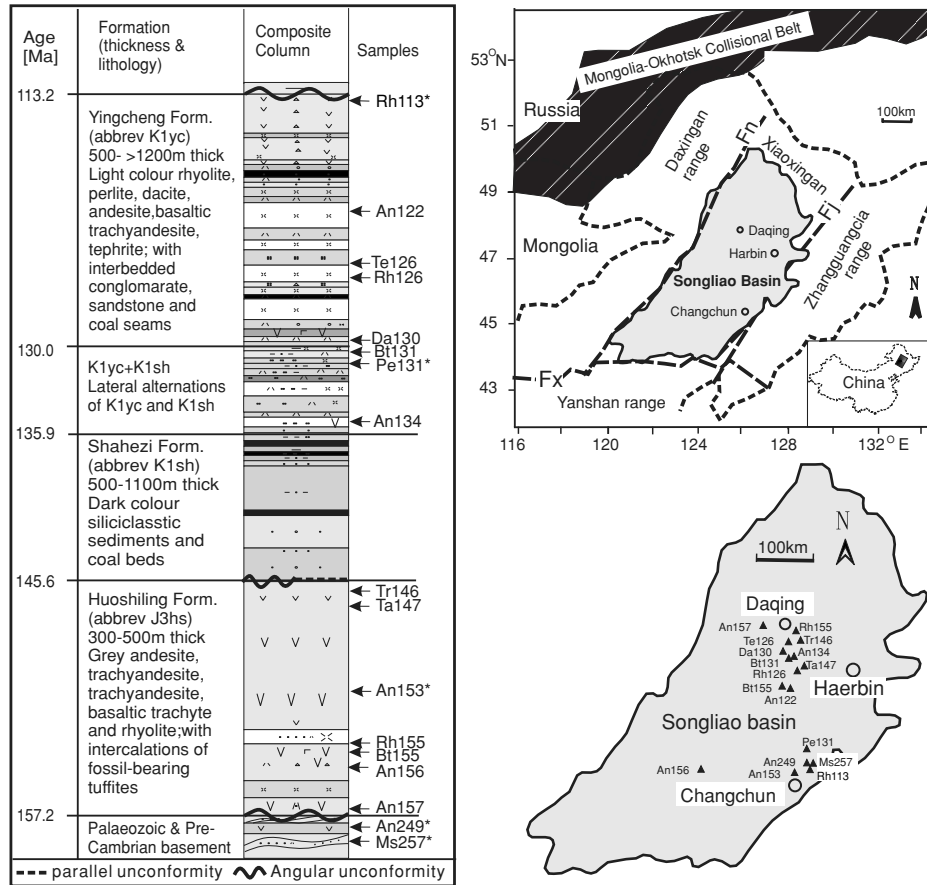


Fig. 1. Map of the Songliao basin, showing stratigraphic column, tectonic setting, and sample locations. Samples come from drillholes and outcrops (those with asterisks). The basin is bounded by Nenjiang fault (Fn), Jiayi fault (Fj) and Xilamulun fault (Fx). The stratigraphic column is compiled from outcrops exposed on the southeast and drill-hole sections in the centre of the basin.

Previous studies performed on the Songliao Basin have focused mainly on stratigraphy, petrology, and geophysical characteristics (Zhu *et al.*, 1997; Cheng *et al.*, 1997; Zhao *et al.*, 1998; Wang *et al.*, 1999; Shan *et al.*, 2000; Wang *et al.*, 2002), studies on isotopic and geochemical signatures of these volcanic rocks are still lacking. This paper presents the first data of geochemical and Nd-Sr-Pb isotopic compositions of the Jurassic and Cretaceous volcanic rocks in the Songliao basin and gives a preliminary interpretation for genesis of the volcanic rocks that are essential for tectonic reconstruction of the NE Asia in Mesozoic.

### GEOLOGICAL SETTING AND SAMPLES

The Songliao basin is situated on the Mongolia-North China block (Fig. 1). To the north, this basin is bounded to the Mongolia-Okhotsk collisional belt. This belt formed when the Mongolia-Okhotsk ocean was closed during early Jurassic to the Jurassic-Cretaceous transition (Zhao

*et al.*, 1990; Sengör and Natal'in, 1996). Magmatism, as well as thrusting and folding, related to this collisional event are widespread throughout Mongolia and easternmost Russia (Zorin, 1999). This long-lived suturing event first started in the west (Mongolia) and ended in the east at the present-day Okhotsk Sea. The Nenjiang and Jiayi fault (Fn and Fj in Fig. 1) separate the basin from the Daxingan and Zhangguangcai mountain ranges, respectively. The southern boundary of the basin is the Xilamulun fault (Fx in Fig. 1) that represents a late Permian suturing between the Mongolia and North China plates (Wang and Fan, 1997; Zhang *et al.*, 1999). The underlying basement is considered to comprise mainly Paleozoic marine metasediments (slates and phyllites), Paleozoic carbonates, andesites and granites, as well as Precambrian gneisses and schists (Wang *et al.*, 1993). However, a recent study shows that the Precambrian rocks are actually absent in the basement beneath the basin and the gneisses and schists are mainly deformed Paleozoic magmatic rocks (Wu *et al.*, 2001).

Table 1. Major (wt.%) and trace element ( $\mu\text{g/g}$ ) compositions, and select ratio of representative volcanic rocks in the Songliao basin, NE China

Element	Detection limit	Rh126	Rh113	Fe131	Dal30	An122	An134	Bt131	Te126	Rh155	Tr146	Ta147	An157	An156	An153	Bt155	Ms257	An249
Rock type		rhyolite	rhyolite	perlite	dacite	andesite	andesite	Basaltic trachy-andesite	tephrite	rhyolite	trachyte	Trachy-andesite	andesite	andesite	Basaltic trachy-andesite	Meta-sediment	andesite	
SiO <sub>2</sub>	1.00	81.80	81.74	72.90	71.02	58.08	60.18	53.98	47.22	75.5	66.08	61.78	60.72	58.24	61.90	52.66	74.16	62.46
Al <sub>2</sub> O <sub>3</sub>	0.05	9.23	9.23	12.06	10.59	12.70	15.79	17.42	13.94	11.19	14.53	16.00	15.41	15.81	17.57	15.98	13.52	15.22
Fe <sub>2</sub> O <sub>3</sub>	0.05	0.13	0.61	0.54	1.26	3.11	1.78	3.58	7.23	0.68	1.75	2.76	2.04	1.34	0.60	1.35	1.23	2.37
FeO	0.04	0.86	0.43	0.24	3.08	5.56	5.70	3.45	7.23	1.66	1.29	1.73	3.24	4.69	3.04	5.45	0.38	2.75
MgO	0.04	0.75	0.44	0.12	3.69	5.46	4.26	4.75	3.41	0.62	3.02	4.07	3.34	3.79	2.49	1.55	0.40	4.92
K <sub>2</sub> O	0.05	3.11	4.21	2.87	2.72	1.67	1.34	1.51	1.60	4.39	4.01	2.52	0.77	1.33	2.49	1.55	4.55	3.05
Na <sub>2</sub> O	0.05	3.62	2.21	4.23	0.87	0.49	4.88	4.06	5.62	1.80	4.50	4.85	4.74	4.58	4.30	3.93	4.13	3.33
CaO	0.05	0.05	0.22	0.69	0.33	2.50	0.39	7.00	0.97	1.05	1.44	3.08	3.81	5.12	4.26	8.18	0.22	2.25
P <sub>2</sub> O <sub>5</sub>	0.01	0.03	0.03	0.01	0.03	0.05	0.06	0.05	0.06	0.07	0.04	0.04	0.18	0.35	0.30	0.04	0.04	0.05
MnO	0.01	0.04	0.03	0.06	0.05	0.20	0.22	0.13	0.19	0.06	0.04	0.09	0.06	0.10	0.11	0.11	0.03	0.09
TiO <sub>2</sub>	0.01	0.04	0.04	0.10	0.10	1.38	1.38	0.88	3.06	0.27	0.44	0.57	0.72	0.76	0.67	1.08	0.22	0.82
LOI	0.50	1.10	0.71	5.96	5.99	8.59	4.75	3.54	13.20	2.06	2.58	2.30	5.40	4.59	4.05	5.47	0.88	2.52
Total		100.76	99.9	99.77	99.73	99.79	100.73	100.35	100.04	99.35	99.72	99.79	100.43	100.23	99.88	99.85	99.76	99.83
La	0.50	60.00	36.45	31.97	73.29	21.94	62.58	38.1	42.25	55.26	26.4	22.76	9.79	19.65	25.91	23.31	58.38	42.45
Ce	1.00	117.80	75.24	51.98	158.30	50.66	121.80	70.86	84.54	92.86	47.65	43.10	17.91	39.40	40.21	43.81	108.10	81.21
Pr	0.10	11.64	8.59	6.11	17.76	4.84	15.64	7.42	9.23	11.25	4.65	3.89	3.18	6.03	3.70	7.55	12.33	9.08
Nd	0.50	43.56	33.71	20.22	66.97	21.33	63.41	28.70	46.45	47.66	19.86	17.06	10.60	19.20	22.56	23.40	47.98	38.46
Sm	0.10	8.65	7.91	3.57	14.90	5.57	15.60	6.37	9.08	8.35	3.44	3.35	2.35	3.83	3.62	4.97	9.90	8.19
Eu	0.005	0.25	0.10	0.17	0.47	1.47	3.28	1.56	1.96	0.44	0.87	0.82	0.57	1.00	0.82	1.13	1.67	1.11
Gd	0.10	5.48	6.80	2.94	12.02	4.78	10.20	4.47	6.16	6.64	2.60	1.95	1.97	2.89	2.60	3.54	6.09	6.01
Tb	0.01	0.93	1.22	0.52	2.06	0.79	1.75	0.69	0.57	1.09	0.34	0.24	0.52	0.65	0.24	1.00	1.05	0.95
Dy	0.01	5.00	7.78	3.11	11.8	4.85	9.34	3.99	6.32	6.43	2.30	1.73	1.58	2.33	2.48	2.94	5.57	5.42
Ho	0.008	0.92	1.48	0.58	2.23	0.89	1.85	0.74	0.96	1.42	0.38	0.29	0.45	0.59	0.39	0.80	1.12	1.05
Er	0.01	2.84	4.64	1.96	5.93	2.73	5.72	2.32	2.73	3.85	1.18	0.89	1.00	1.37	1.22	1.78	3.51	3.19
Tm	0.008	0.42	0.66	0.28	0.97	0.37	0.77	0.32	0.62	0.62	0.16	0.11	0.23	0.26	0.08	0.43	0.53	0.43
Yb	0.005	2.72	4.32	1.89	5.62	2.16	4.94	1.96	2.04	4.05	1.07	0.79	0.92	1.29	1.14	1.51	3.46	3.00
Lu	0.005	0.37	0.60	0.30	0.77	0.31	0.76	0.30	0.21	0.54	0.14	0.10	0.17	0.19	0.14	0.25	0.50	0.42
Y	0.005	24.50	39.60	16.02	65.11	25.65	49.87	20.69	33.48	35.65	11.48	9.76	8.98	13.56	12.62	16.24	31.03	28.01
Rb	0.01	24.20	181.00	155.00	151.00	132.80	43.50	67.20	95.90	112.60	84.50	76.90	15.20	21.30	110.90	27.00	129.70	151.30
Ba	0.08	530	125	95	790	370	170	180	280	780	1030	900	270	720	880	620	1380	580
Th	0.10	14.50	16.00	9.40	18.00	10.50	9.10	15.00	13.50	3.00	18.00	22.00	45.00	9.80	5.00	67.00	11.50	12.50
U	0.10	0.99	3.11	3.94	7.97	0.74	1.55	2.77	1.53	3.50	1.94	2.18	0.43	1.12	2.16	0.87	2.82	2.66
Pb	2.30	13.03	22.99	40.54	50.47	7.04	21.87	34.1	26.1	21.29	27.98	34.22	19.63	10.39	7.56	48.37	8.68	16.4
Nb	0.50	14.0	32.0	29.5	70.0	22.0	41.0	32.0	45.0	44.0	11.0	10.0	11.0	8.5	18.0	20.0	12.5	17.5
Sr	0.05	1023.83	7.67	88.40	257.05	199.65	209.67	501.58	275.04	260.30	671.68	685.57	527.79	1052.70	458.12	966.04	48.81	461.06
Zr	0.22	1.50	560	160	1000	195	450	190	220	460	190	130	150	160	230	245	260	150
Ni	1.10	39	5.9	6.8	5.9	100	8.1	3.7	6.4	13	35.5	100	69	55	17.5	81	8.4	57
Cr	0.58	77	11.5	23	5.2	175	6.9	9.9	8.9	27	71	280	135	235	48	250	8.4	56
Rb/Sr		0.024	23.598	1.753	0.587	0.665	0.207	0.134	0.349	0.433	0.126	0.112	0.029	0.020	0.242	0.028	2.657	0.328
Sm/Nd		0.199	0.235	0.177	0.222	0.261	0.246	0.222	0.195	0.175	0.173	0.196	0.222	0.199	0.160	0.212	0.206	0.213
Th/U		14.65	5.14	2.39	2.26	14.19	5.87	5.42	8.82	0.86	9.28	10.09	104.65	8.75	2.31	77.01	4.08	0.21
Eu/Eu*		0.10	0.04	0.16	0.10	0.85	0.75	0.85	0.76	0.17	0.86	0.90	0.79	0.88	0.78	0.79	0.61	0.46
Mg*-value		0.61	0.65	0.47	0.68	0.64	0.57	0.71	0.46	0.40	0.81	0.81	0.65	0.57	0.24	0.55	0.65	0.76

Both Fe(II) and Fe(III) are analysed results of volumetric methods. Mg\*-value =  $\text{MgO}/(\text{MgO} + \text{FeO})$  in mole and exclusive of  $\text{Fe}_2\text{O}_3$ . Eu/Eu\* is chondrite (Taylor and McLennan, 1985) normalized ratio of  $\text{Eu}/(\text{Sm} + \text{Gd})/2$ .

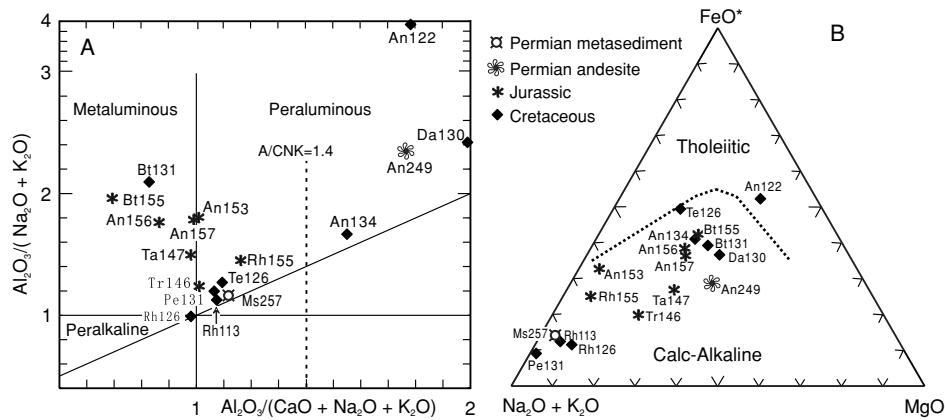


Fig. 2. Suites of representative volcanic rocks of the Songliao basin. A: Shand's index (Maniar and Piccoli, 1989); B: AFM plot, in weight percent of oxides,  $FeO^* = FeO + 0.8998Fe_2O_3$  (Irvine and Barager, 1971).

The Songliao Basin is predominantly composed of volcanic rocks of late Jurassic and early Cretaceous age (Wang *et al.*, 2002). The thickness of the volcanic succession ranges from 1300 m to 2800 m as revealed by the drilling. It comprises most of the lower part of the basin fill (Wang *et al.*, 1993; Wang *et al.*, 1996). The volcanic rocks are overlain by an Albian to Maastrichtian sedimentary sequence of up to 6000 m in thickness (Gao, 1995; Wang *et al.*, 1996).

A geological reconnaissance of the Mesozoic volcanic succession within and around the Songliao Basin has been recently carried out based on the outcrops and related drill cores. The sampling in this study benefited from unpublished maps of the distribution of the Mesozoic volcanic rocks summarized in an unpublished report by the Daqing Oil Company. According to the temporal and spatial distribution of the volcanic rocks, seventeen representative samples are chosen for geochemical and isotopic analyses, which were collected from outcrops and drillholes of the basin as well (localities see Fig. 1). The ages of these volcanic rocks have been constrained by available  $^{40}Ar/^{39}Ar$  and K/Ar data (Wang *et al.*, 2002). For a comparison with the Mesozoic volcanic rocks, a Permian marine metasediment sample (sample Ms257) and an intercalated andesite (sample An249) within the Permian metasediments were also collected for analysis, as the upper crust of the study area consists predominantly of the Permian metasediments (Jilin Geological Survey, 1988; Heilongjiang Geological Survey, 1993).

The Jurassic volcanic rocks are composed of rhyolite, andesite, trachyte, trachyandesite and basaltic trachyandesite, while the Cretaceous rocks are rhyolite, perlite, dacite, andesite, basaltic trachyandesite and tephrite (after classification of LeMaitre *et al.*, 1989). All these volcanic rocks are porphyritic and phenocryst-poor (less than 5%), except the Jurassic rhyolite containing

phenocryst up to 30%. The phenocryst assemblages are complex, commonly with quartz, feldspar (sanidine, anorthoclase and plagioclase), biotite, hornblende, magnetite, ilmenite and pyroxene. Cumulophyric intergrowth is common amongst the phenocrysts.

#### ANALYTICAL METHODS

Major elements were determined by chemical methods and trace elements were analyzed by X-ray fluorescence technique at the analytical centre of the Jilin University, China. Rare earth elements (REE) were determined with an Inductively Coupled Plasma-Atomic Emission Spectrometry (ICP-AES) at Jilin Institute of Geology, China. Detection limits of the analysed elements are given in Table 1. Analytical precision (standard deviation) was <5% for trace and rare earth elements. Concentrations of Sm, Nd, Rb, Sr, Th, U and Pb were analyzed using dilution method and isotopic compositions of Sr, Nd, Pb and O were measured using Finnigan MAT262 and MAT252 mass spectrometers at Universität Tübingen, Germany. Analytical procedures are outlined in Chen *et al.* (2000).  $^{143}Nd/^{144}Nd$  ratios are normalized to  $^{146}Nd/^{144}Nd = 0.7219$  and Sm isotopic ratios to  $^{147}Sm/^{152}Sm = 0.56081$ .  $^{87}Sr/^{86}Sr$  ratios are normalized to  $^{86}Sr/^{88}Sr = 0.1194$ . Isotopic analyses of the Ames Nd standard yielded  $^{143}Nd/^{144}Nd = 0.512135 \pm 10$  ( $2\sigma$ ,  $n = 3$ ) and the NBS 987 Sr standard yielded  $^{87}Sr/^{86}Sr = 0.710256 \pm 10$  ( $2\sigma$ ,  $n = 5$ ). The Pb standard NBS 981 was measured for the determination of the thermal fractionation of Pb isotopes, and the isotopic ratios were corrected for 0.11% fractionation per atomic mass unit. For the measurement of O isotopes, about 95–100% of oxygen was yielded at a reaction temperature of 550°C (Clayton and Maveda, 1963). The ratios are reported in the  $\delta$ -notation relative to Vienna Standard Mean Ocean Water (V-SMOW). Pre-

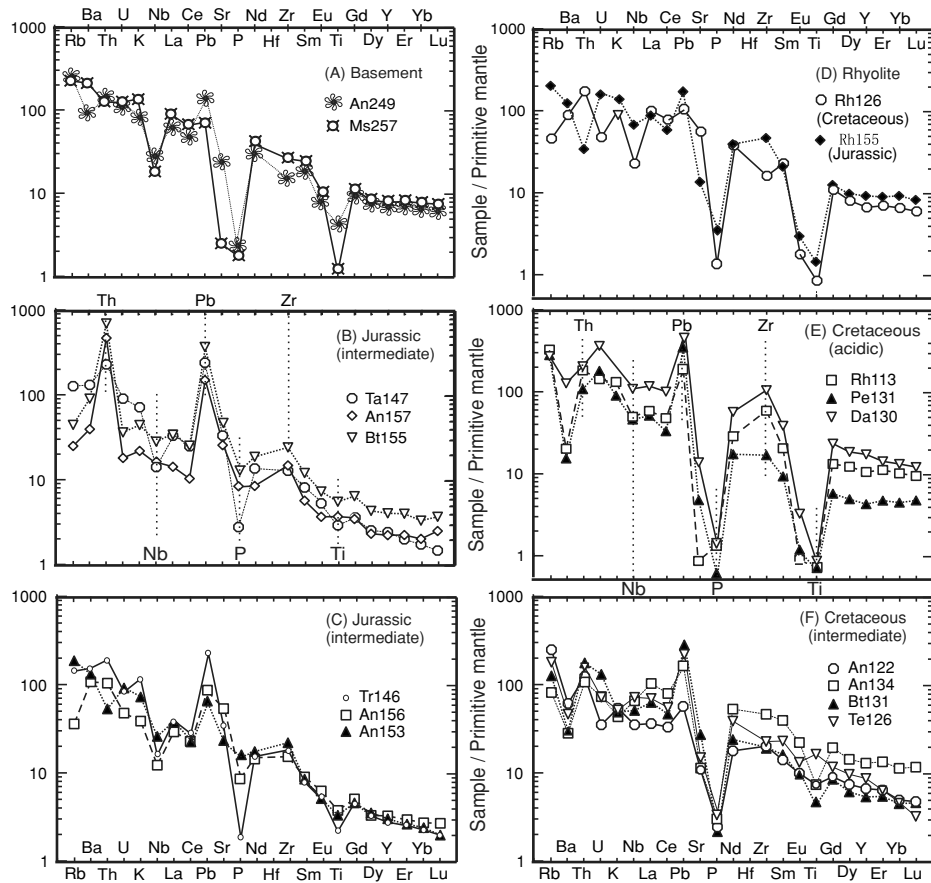


Fig. 3. Primitive mantle-normalized distribution diagrams for the Mesozoic volcanic rocks of the Songliao basin. Normalization values after Sun and McDonough (1989).

cision is better than  $\pm 0.1\%$  based on replicate analyses of both in-house standard (NCSU quartz,  $\delta^{18}\text{O} = 11.6\%$ ) and samples.

### ANALYTICAL RESULTS

Major and trace element data are given in Table 1. Volcanic rocks from both the Jurassic and Cretaceous are wide ranging in composition, covering peraluminous and/or metaluminous, high-K and/or medium-K, and potassic calc-alkaline. Tholeiitic sample An122 (Fig. 2B) might be altered since it has low  $\text{Na}_2\text{O}$  and high LOI contents. Primitive mantle normalized trace element data are plotted in order of decreasing incompatibility from left to right (Fig. 3). The normalized patterns show that the rocks are enriched in incompatible elements. Most of the samples have negative anomalies in high field strength elements like Nb, Ti and P. Not significant anomalies in Zr and Y can be observed in almost all the studied samples. All the samples (Fig. 3) show positive Pb anomaly. Negative anomalies of Sr can be observed for all the Cretaceous

volcanic rocks (Figs. 3D, 3E and 3F), whereas the Jurassic volcanic rocks exhibit positive anomalies of Sr (Figs. 3B and 3C) except for the rhyolites (Fig. 3D). The Cretaceous volcanic rocks show negative anomalies of Ba similar to Sr (Figs. 3E and 3F), but the Ba-content of the Jurassic volcanic rocks vary irregularly from each other. Some intermediate volcanic rocks show significant positive Th anomaly (Figs. 3B and 3F). Chondrite-normalized rare earth element patterns show distinct fractionation between light rare earth elements (LREE) and heavy rare earth elements (HREE) in the analyzed samples (Fig. 4), indicated by the values of  $\text{La}_\text{N}/\text{Sm}_\text{N}$  ratio ranging from 2.48 to 5.64 (mean 3.62) and the values of  $\text{Gd}_\text{N}/\text{Yb}_\text{N}$  ratio ranging from 1.26 to 2.48 (mean 1.73). All the acidic volcanic rocks show significant negative Eu anomaly regardless of geological age (Fig. 4C), but intermediate rocks show minor negative Eu anomaly with  $\text{Eu}/\text{Eu}^*$  values ranging from 0.61 to 0.90 (Table 1).

Analytical data of Nd, Sr, Pb and O isotopes of representative samples are given in Table 2. The Jurassic volcanic rocks have initial  $^{87}\text{Sr}/^{86}\text{Sr}$  ratio from 0.70338 to

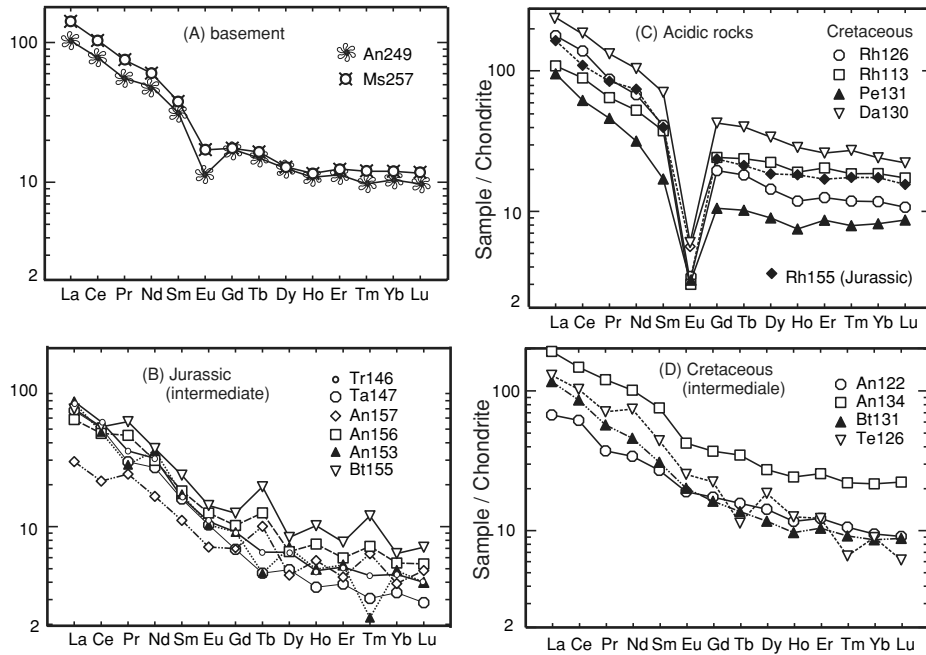


Fig. 4. Chondrite-normalized REE plots for the Mesozoic volcanic rocks of the Songliao basin. Normalization values after Sun and McDonough (1989).

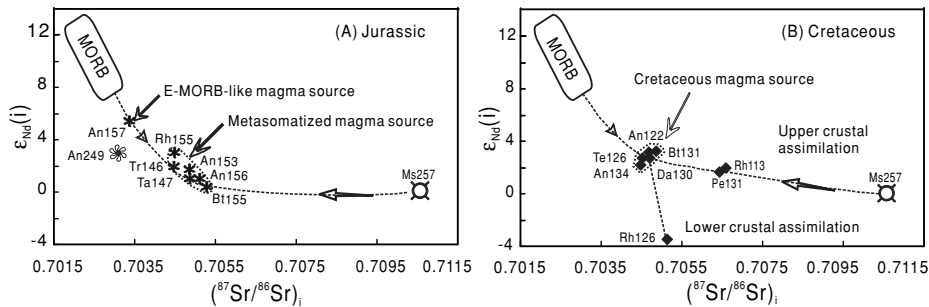


Fig. 5. Nd- and Sr-isotope compositions of representative volcanic rocks of the Songliao basin. Sample An249 is the Permian oceanic andesite. Sample Ms257 is the Permian metasediment. MORB: mid-ocean ridge basalt (Cohen and O'Nions, 1982), dash lines include E-MORB-source.

0.70528, while the Cretaceous volcanic rocks have slightly higher initial  $^{87}\text{Sr}/^{86}\text{Sr}$  ratio from 0.70448 to 0.70660. The Permian metasediment sample Ms257 yields a high initial  $^{87}\text{Sr}/^{86}\text{Sr}$  ratio of 0.71055. The analyzed samples show considerable variation in initial  $\epsilon_{\text{Nd}}$  value. The Jurassic andesite (sample An157) collected from western Songliao basin has an initial  $\epsilon_{\text{Nd}}$  value of +5.3 corresponding to a low initial  $^{87}\text{Sr}/^{86}\text{Sr}$  value of 0.70338. This sample has similar Nd-Sr isotopic composition to the Permian oceanic andesite sample An249 (Fig. 5A). The Cretaceous rhyolite sample Rh126 has low initial  $\epsilon_{\text{Nd}}$  value of -3.4 at a initial  $^{87}\text{Sr}/^{86}\text{Sr}$  ratio of 0.70513 (Fig. 5B), while initial  $\epsilon_{\text{Nd}}$  values range from 0.4 to 3.1 for the other Jurassic

volcanic rocks and from 1.6 to 3.2 for the other Cretaceous volcanic rocks. The analyzed samples yielded Pb isotopic composition from 17.65 to 18.22 for initial  $^{206}\text{Pb}/^{204}\text{Pb}$  ratio, 15.52 to 15.57 for initial  $^{207}\text{Pb}/^{204}\text{Pb}$  ratio, and 36.46 to 38.21 for initial  $^{208}\text{Pb}/^{204}\text{Pb}$  ratio, plotted in the field between the depleted mantle and bulk silicate earth (Fig. 8; Brownlow, 1996). The analyzed samples show a large variation in oxygen isotope composition with  $\delta^{18}\text{O}$ -values ranging from 3.24‰ to 14.77‰. The volcanic rocks and the Permian metasediment and andesite as well are characterized by young Nd-model ages ranging from 1000 and 400 Ma. The Jurassic andesite (An157) has the youngest Nd-model age of 400 Ma.

**MAGMA SOURCE OF THE JURASSIC AND  
CRETACEOUS VOLCANIC ROCKS**

According to the Jilin Geological Survey (1988) and Heilongjiang Geological Survey (1993), the Permian andesite is interbedded with deep marine sediments and may represent an island arc volcanic rock. This interpretation seems to be supported by the andesite sample An249 that has high initial  $\epsilon_{Nd}$  value of 3.4 and  $Mg^*$ -value of 0.76. Nevertheless, the magma must have experienced mixing or contamination of crustal material as indicated by its negative anomalies of Nb, Ti, Zr and P as well as Sr and Ba (Fig. 3A; cf., Benito *et al.*, 1999). Negative Eu-anomaly of this sample can be attributed to fractional crystallization of plagioclase. Sr and Nd isotopic compositions of the Jurassic andesite (sample An157) are similar to that of the Permian oceanic andesite (Fig. 5A). The former also has a high  $Mg^*$ -value of 0.65 and is further characterized by low  $^{87}Sr/^{86}Sr$  and high  $^{143}Nd/^{144}Nd$  ratios, compared with other Jurassic volcanic rocks. Like the Permian andesite, the Jurassic andesite (sample An157) could derive directly from an E-MORB-like magma source. This interpretation can be supported by regional tectonic settings. A mid-Jurassic ophiolite has been recognized in the adjacent area of the Songliao basin (Zhao *et al.*, 1996), indicating the occurrence of subduction prior to the late Jurassic volcanism in the region.

In the Nd-Sr diagram (Fig. 5A), all the Jurassic volcanic rocks are plotted between the MORB area and sediments probably represented by the Permian metasediment (sample Ms257). If the Permian metasediment (Ms257) is used as one of the end members, the subducted sediment, and model compositions of mantle and MORB of Taylor and McLennan (1985) are considered for the other end member, a mass ratio of MORB/subducted sediment for the magma source can be estimated at about 16:1 to 10:1. However, no simple correlation can be observed between the volcanic rocks and the MORB/subducted sediments in the  $(^{87}Sr/^{86}Sr)_i$  vs.  $(^{206}Pb/^{204}Pb)_i$  plot (Fig. 8). This can be caused by different mobility of Pb, Th, and U during the subduction of oceanic crust and sediments (Allegre *et al.*, 1986; Fontignie and Schilling, 1996; Chen *et al.*, 2002). Another case is that the subducted sediments have more variant Pb composition than the Permian metasediment (Ms257). The Jurassic volcanic rocks have more heterogeneous Pb isotopic composition than the Cretaceous ones. A negative correlation between initial  $^{87}Sr/^{86}Sr$  ratios and magmatic differentiation index (Fig. 6A) suggests that magmas of the Jurassic volcanic rocks escaped from contamination by crustal material during the magma ascending. The Jurassic andesite (sample An157) and the Permian oceanic andesite are plotted far from the other Jurassic samples (Fig. 6A), suggesting a derivation from a separate magma source. Sample An157 also shows unique el-

Table 2. Measured (m) and initial (i) isotopic compositions of representative volcanic rocks in the Songliao basin, NE China

Sample	$(^{206}Pb/^{204}Pb)_m$	$(^{207}Pb/^{204}Pb)_m$	$(^{208}Pb/^{204}Pb)_m$	$(^{206}Pb/^{204}Pb)_m$	$(^{207}Pb/^{204}Pb)_m$	$(^{208}Pb/^{204}Pb)_m$	$(^{206}Pb/^{204}Pb)_i$	$(^{207}Pb/^{204}Pb)_i$	$(^{208}Pb/^{204}Pb)_i$	$(^{87}Rb/^{86}Sr)_m$	$(^{87}Sr/^{86}Sr)_m$	$(^{87}Sr/^{86}Sr)_i$	$(^{147}Sm/^{144}Nd)_m$	$(^{143}Nd/^{144}Nd)_m$	$(^{143}Nd/^{144}Nd)_i$	$\epsilon_{Nd}$	Nd model ages [Ga]	$\delta^{18}O$
Rh126	18.089	15.529	38.039	18.00	15.52	37.53	18.00	15.52	37.53	0.07	0.705248	0.70513	0.1141	0.512394	0.512300	-3.4	1.0	10.87
Rh113	18.394	15.560	38.278	18.21	15.55	37.94	18.21	15.55	37.94	69.20	0.814860	0.70660	0.1396	0.512709	0.512586	2.4	1.0	9.54
Pe131	18.052	15.564	37.975	17.92	15.56	37.86	17.92	15.56	37.86	5.07	0.715870	0.70643	0.1103	0.512643	0.512542	1.6	0.6	14.77
Da130	18.345	15.554	38.193	18.14	15.54	38.03	18.14	15.54	38.03	1.70	0.707841	0.70470	0.1335	0.512723	0.512609	2.7	0.6	6.67
An122	18.350	15.546	38.220	18.22	15.54	37.56	18.22	15.54	37.56	1.92	0.708017	0.70468	0.1430	0.512756	0.512642	3.1	0.6	
An134	18.171	15.544	38.025	18.08	15.54	37.82	18.08	15.54	37.82	0.60	0.705626	0.70448	0.1218	0.512685	0.512578	2.2	0.6	7.30
Bh131	18.118	15.563	38.033	18.01	15.56	37.83	18.01	15.56	37.83	0.39	0.705587	0.70487	0.1330	0.512751	0.512637	3.2	0.6	5.14
Te126	17.963	15.576	37.961	17.89	15.57	37.73	17.89	15.57	37.73	1.01	0.706320	0.70451	0.1239	0.512716	0.512614	2.7	0.6	3.24
Rh155	18.457	15.541	38.287	18.20	15.53	38.21	18.20	15.53	38.21	1.25	0.707237	0.70448	0.1159	0.512713	0.512596	3.1	0.5	9.65
Tr146	17.888	15.558	37.866	17.79	15.55	37.53	17.79	15.55	37.53	0.36	0.705233	0.70448	0.1211	0.512666	0.512550	2.0	0.6	4.26
Ta147	17.849	15.569	37.846	17.76	15.56	37.51	17.76	15.56	37.51	0.32	0.705542	0.70486	0.1133	0.512612	0.512503	1.0	0.7	6.86
An157	17.679	15.576	37.754	17.65	15.57	36.46	17.65	15.57	36.46	0.08	0.703562	0.70338	0.1369	0.512848	0.512706	5.3	0.4	10.16
An156	18.387	15.552	38.187	18.22	15.54	37.65	18.22	15.54	37.65	0.06	0.705236	0.70511	0.1238	0.512614	0.512488	1.0	0.7	8.22
An153	18.437	15.555	38.257	18.01	15.53	37.89	18.01	15.53	37.89	0.70	0.706364	0.70484	0.1124	0.512638	0.512526	1.8	0.6	11.68
Bh155	18.076	15.567	38.005	18.05	15.57	37.23	18.05	15.57	37.23	0.08	0.705453	0.70528	0.1220	0.512584	0.512460	0.4	0.8	
Ms257	18.758	15.577	38.743	17.92	15.53	37.49	17.92	15.53	37.49	7.71	0.738737	0.71055	0.1087	0.512486	0.512303	-0.1	0.8	4.00
An249	18.417	15.552	38.270	18.01	15.53	37.58	18.01	15.53	37.58	0.95	0.70651	0.70315	0.1237	0.5127	0.5125	3.4	0.8	4.81

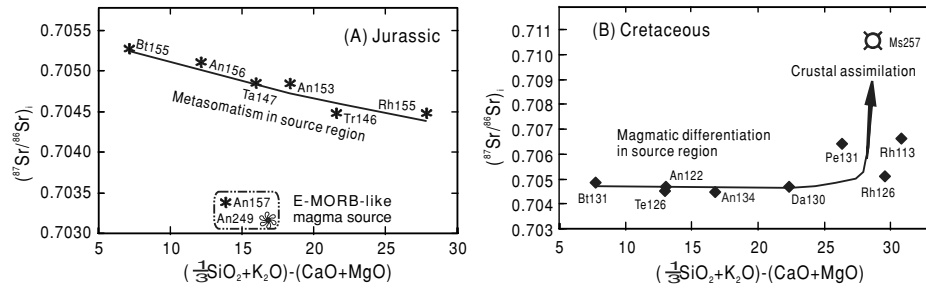


Fig. 6. Sr isotope ratios for the volcanic rocks of the Songliao basin plotted against magmatic differentiation index (MDI; Gast et al., 1964).

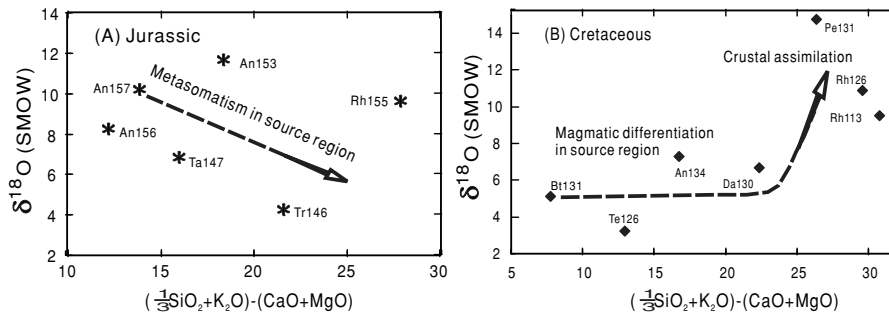


Fig. 7.  $\delta^{18}\text{O}$  values (in ‰ relative to V-SNOW) versus MDI (Gast et al., 1964) plots of the volcanic rocks of the Songliao basin.

ement signatures, such as no negative Nb- and Ti-anomaly and minor positive Zr-anomaly, likely implying high fraction of MORB component in the magma source.

The Nd-Sr isotopic composition shows that both the Jurassic and Cretaceous volcanic rocks fit in mixing curve of two components (Figs. 5A and 5B). However, there are differences between the volcanic rocks forming in different magma episodes. Most of the Cretaceous volcanic rocks are more homogeneous than the Jurassic volcanic rocks, as indicated in Sr, Nd, Pb, and O isotopic compositions and geochemical compositions of the analyzed samples. Nb/Y ratios range from 0.63 to 1.43 for the Jurassic andesite but from 0.82 to 0.84 for the Cretaceous andesite. It is commonly accepted that variation in the values of Nb/Y ratio can be attributed to the heterogeneity of magma source (e.g., Elburg and Foden, 1999). A mean value of initial  $^{87}\text{Sr}/^{86}\text{Sr}$  ratio of 0.70484 is obtained from six Jurassic samples (Fig. 5A) and 0.70465 from five Cretaceous samples (Fig. 5B). The Jurassic volcanic rocks have lower initial  $\epsilon_{\text{Nd}}$ -values than the Cretaceous ones (mean values of 1.55 and 2.78, respectively). Contribution of crustal component is less important in the Cretaceous mafic to intermediate volcanic rocks than in the Jurassic ones. This can be supported by the negative anomalies of Ba and Sr in the Cretaceous volcanics (Figs. 3E and 3F). The Cretaceous acid

volcanic rocks seem to be slightly contaminated by crustal material during the magma ascending. Differences in oxygen and Sr isotopic signatures between the Jurassic and Cretaceous volcanic rocks can be obviously observed in Figs. 6 and 7. Magmatic differentiation in source region is clearly indicated in basaltic trachyandesite, tephrite, andesite, and dacite, while rhyolites show contamination in some extent. Rhyolite sample Rh126 has low initial  $\epsilon_{\text{Nd}}$ -value and Rb/Sr ratio but high  $\delta^{18}\text{O}$  value, probably suggesting lower crustal assimilation (e.g., Brownlow, 1996). Sample Tr146 has lower  $\delta^{18}\text{O}$  value (4.26‰) can imply later imprint by meteoric water. The Jurassic and Cretaceous volcanic rocks have similar Pb isotopic composition (Fig. 8), showing involvement of MORB material in the magma sources.

#### PETROGENESIS AND POSSIBLE TECTONIC SETTING

Possible petrogenesis for the Jurassic and Cretaceous volcanic rocks exposed in the Songliao basin is summarized in a sketch diagram (Fig. 9) for further discussion below. As shown above, geochemical and isotopic characteristics are different for the Jurassic and Cretaceous magma sources. There were probably two types of primary magmas for the Jurassic volcanic rocks: an E-MORB-like and a metasomatized one. The former is char-



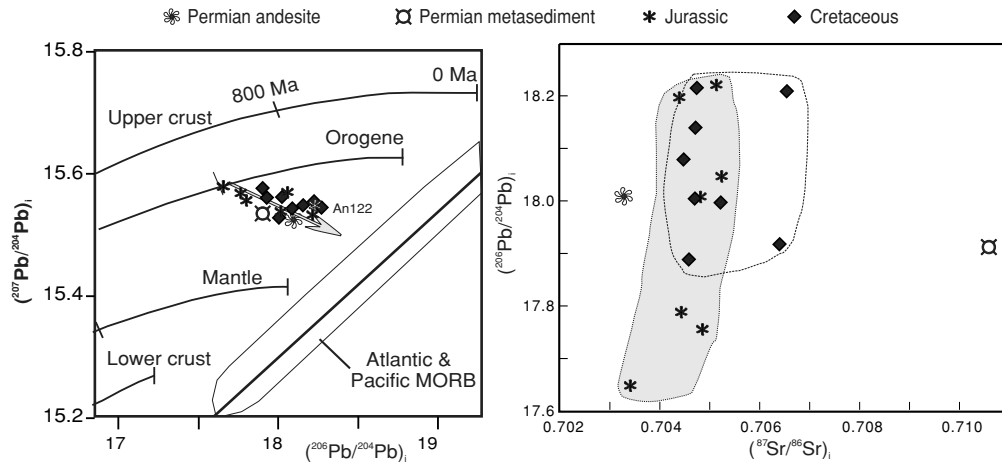


Fig. 8.  $^{207}\text{Pb}/^{204}\text{Pb}$  versus  $^{206}\text{Pb}/^{204}\text{Pb}$  ratios for the volcanic rocks of the Songliao basin. Reference lines after Doe and Zartman (1979). MORB is shown for comparison (Mukasa *et al.*, 1994).

acterized by high initial  $\epsilon_{\text{Nd}}$  values and low  $^{87}\text{Sr}/^{86}\text{Sr}$  ratios, while the latter exhibit Sr-Nd isotopic composition similar to the bulk earth. For the Cretaceous volcanic rocks, only one type of primary magma source can be observed, which is characterized by moderate initial  $\epsilon_{\text{Nd}}$ -value and  $^{87}\text{Sr}/^{86}\text{Sr}$  ratio. Nevertheless, it is very possible that two secondary magma chambers formed in the upper and lower crust. This interpretation may be supported by the fact that there are several layers of low seismic velocity ( $V_p < 6.0$  to  $6.4$  km/s) and low electric resistivity (3 to 8  $\Omega\text{m}$ ) between depth range of 10 to 30 km under the Songliao basin (Zhang *et al.*, 1998; Yang *et al.*, 1999).

Previous explanations on the tectonic setting for the formation of the volcanism in the Songliao basin can be summarized in either continental rifting or subduction-related model. However, either tectonic model has to consider following observations: (a) The youngest recognized ophiolite complex, east of the Songliao basin, dated at  $169 \pm 6$  Ma, represents part of a middle Jurassic suture of the Mongolia-Okhotsk belt (Zhao *et al.*, 1996). By the mean of palaeotectonic reconstruction, Sengör and Natal'in (1996) have shown that the collision at the Mongolia-Okhotsk suture should have lasted from early Jurassic to the Jurassic-Cretaceous transition and ended before Albian. (b) A thick coal-bearing clastic sequence formed during late Jurassic and early Cretaceous (Wang *et al.*, 2002). The interbedded volcano-clastic succession is distributed approximately parallel to the Mongolia-Okhotsk suture zone. On top of the succession exists a regional hiatus above that is a basin-wide, oil-bearing sedimentary sequence up to 6000 m of NNE-strike (Wang *et al.*, 1993), suggesting a sharp change of the tectonic regime. (c) Geochemical and isotopic characteristics of the volcanic rocks show mixture signature of MORB and crustal material, similar to volcanic rocks forming in arc

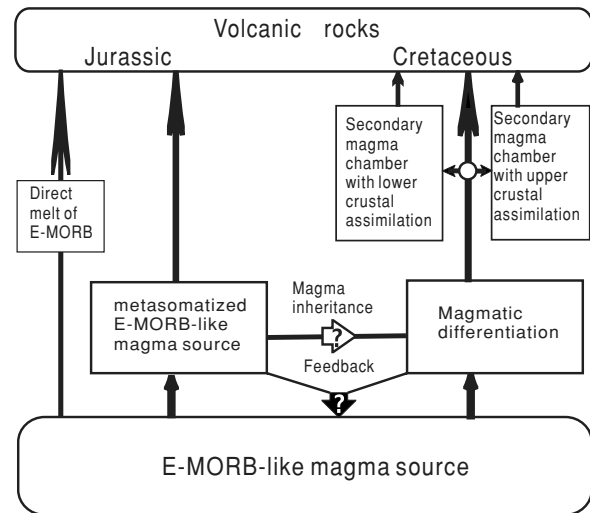


Fig. 9. Schematic interpretation of the Mesozoic magmatism beneath the Songliao basin.

settings (e.g., Hess, 1989). (d) Significant differences in geochemical and isotopic compositions between the Jurassic to Cretaceous volcanic rocks shows increasing involvement of MORB material with time, probably suggesting a decreasing influence of subduction component on the magma sources. Although the sedimentary sequence overlying the Jurassic and Cretaceous volcanic succession, which formed in different tectonic setting, is commonly accepted to be controlled by the subduction of the Pacific plate (e.g., Wang *et al.*, 1993; Gao, 1995), this tectonic event can hardly explain the formation of the volcanogenic succession under the heretofore observations. In this case, we favor a post-collisional setting for the enormous Jurassic—Cretaceous volcanic activity,

as the collision along the Mongolia-Okhotsk suture ended about 10 Ma earlier than the volcanism in the Songliao basin.

**Acknowledgments**—This study was supported by the NSFC (No. 40372066) and the SRFDP (No. 20030183042) and attained with the assistance of the AvH of Germany. Wang is grateful to G. Einsele, P. Grathwohl and C. McDermott for kind help during the AvH stay in Tübingen. Thanks are due to J. Geldmacher and an anonymous reviewer for constructive suggestions, T. Barry, G. L. Farmer, and F.-Y. Wu for valuable criticism on an early version of the manuscript, S. Mattern for English improvement, and S.-B. Sun, X.-L. Shan, W.-H. Bian, and W.-Z. Liu for assistance during this study.

## REFERENCES

- Allegre, C. J., Dupre, B. and Lewin, E. (1986) Thorium/Uranium ratio of the Earth. *Geol. Chem.* **56**, 219–227.
- Benito, R., Lopez-Ruiz, J., Cebria, J. M., Hertogen, J., Doblas, M., Oyarzum, R. and Demaiffe, D. (1999) Sr and O isotope constrains on source and crustal contamination in high-K calc-alkaline and shoshonitic neogene volcanic rocks of SE Spain. *Lithos* **46**, 773–802.
- Brownlow, A. H. (1996) *Geochemistry*. Prentice-Hall, New Jersey, 436 pp.
- Chen, F., Hegner, E. and Todt, W. (2000) Zircon ages and Nd isotopic and chemical compositions of orthogneisses from the Black Forest, Germany: evidence for a Cambrian magmatic arc. *Int. J. Earth Sci.* **88**, 791–802.
- Chen, F., Satir, M., Ji, J. and Zhong, D. (2002) Nd-Sr-Pb isotopic composition of the Cenozoic volcanic rocks from western Yunnan, China: evidence for enriched mantle source. *J. Asian Earth Sci.* **21**, 39–45.
- Cheng, R.-H., Liu, Z.-J. and Wang, P.-J. (1997) Volcanic events on the east margin of the Songliao basin and their geological significance. *J. China Univ. Geosci.* **22**, 57–62 (in Chinese with English abstract).
- Cheng, Y.-Q., Sheng, Y.-H. and Ma, Q.-Y. (1990) *Geological Map of China*. Geology Press, Beijing.
- Clayton, R. N. and Mayeda, T. K. (1963) The use of bromine pentafluoride in the extraction of oxygen from oxides and silicates for isotope analysis. *Geochim. Cosmochim. Acta* **27**, 43–52.
- Cohen, R. S. and O’Nions, R. K. (1982) The lead, neodymium and strontium isotopic structure of ocean ridge basalts. *J. Petrol.* **23**, 299–324.
- Doe, B. R. and Zartman, R. E. (1979) *Plumbotectonics. Geochemistry of Hydrothermal Ore Deposit* (Barnes, H. L., ed.), 22–70, Wiley, London.
- Elburg, M. A. and Foden, J. (1999) Geochemical response to varying tectonic settings: An example from southern Sulawesi (Indonesia). *Geochim. Cosmochim. Acta* **63**, 1155–1172.
- Fontignie, D. and Schilling, J.-G. (1996) Mantle heterogeneities beneath the South Atlantic: a Nd-Sr-Pb isotope study along the Mid-Atlantic ridge (3°S–46°S). *Earth Planet. Sci. Lett.* **142**, 209–221.
- Gao, R.-Q. (1995) *Petroleum Stratigraphy of the Songliao Basin*. Heilongjiang Sci. Technol. Press, Haerbin, 385 pp. (in Chinese).
- Gast, P. W., Tilton, G. R. and Hedge, C. (1964) Isotopic composition of lead and strontium from Ascension and Gough islands. *Science* **145**, 1181–1185.
- Harangi, S. (1994) Geochemistry and petrogenesis of the early Cretaceous continental rift-type volcanic rocks of the Mecsek Mountains, South Hungary. *Lithos*, **33**, 303–321.
- Heilongjiang Geological Survey (1993) *Regional Geology of Heilongjiang Province of China*. Geology Press, Beijing, 734 pp. (in Chinese).
- Hess, P. C. (1989) *Origins of Igneous Rocks*. Harvard Univ. Press, Massachusetts, 146–166.
- Irvine, T. N. and Barager, W. R. A. (1971) A guide to the chemical classification of the common volcanic rocks. *Can. J. Earth Sci.* **8**, 523–548.
- Jilin Geological Survey (1988) *Regional Geology of Jilin Province of China*. Geology Press, Beijing, 698 pp. (in Chinese).
- LeMaitre, R. W., Bateman, P., Dudek, A., Keller, J., Lameyre, M. J., Lebas, M. J., Sabine, P. A., Schmid, R., Sorensen, H., Streckeisen, A., Wooley, A. R. and Zanettin, B. (1989) *A Classification of Igneous Rocks and Glossary of Terms*. Blackwell, London, 193 pp.
- Liu, D.-L. and Ma, L. (1998) Relation between pre-rift volcanics and the rift basin and geodynamic processes. *Geol. Rev.* **44**(2), 130–135 (in Chinese with English abstract).
- Liu, Z.-J., Wang, D.-P., Liu, L., Liu, W.-Z., Wang, P.-J. and Du, X.-D. (1993) Sedimentary characteristics of the Cretaceous Songliao Basin. *Acta Geologica Sinica* (English edition), **6**, 167–180.
- Maniar, P. D. and Piccoli, P. M. (1989) Tectonic discrimination of granitoids. *GSA Bulletin* **101**, 635–643.
- Mukasa, S. B., Flower, M. F. J. and Miklius, A. (1994) The Nd-, Sr- and Pb-isotopic character of lava from Taal, Laguna de Bay and Arayat volcanoes, S.W. Luzon, Philippines: implications for arc magma petrogenesis. *Tectonophysics* **235**, 205–221.
- Scotese, C. R., Gahagan, L. and Larson, R. L. (1988) Plate tectonic reconstruction of the Cretaceous and Cenozoic ocean basins. *Tectonophysics* **155**, 27–48.
- Sengör, A. M. C. and Natal’in, B. A. (1996) Pelaeotectonics of Asia: fragments of a synthesis. *The Tectonic Evolution of Asia* (Yin, A. and Harrison, M., eds.), 486–640, Cambridge Univ. Press, London.
- Shan, X.-L., Wang, P.-J., Xu, W.-L., Chen, S.-M. and Song, W.-H. (2000) Cycles and phases of the Ceo-Mesozoic volcanics in the main sedimentary basins of eastern China continental margin. *J. Changchun Univ. Sci. Techn.* **30** (Suppl.), 14–45 (in Chinese).
- Sun, S. S. and McDonough, W. F. (1989) Chemical and isotopic systematics of oceanic basalts: implications for mantle composition and processes. *Magmatism in the Ocean Basins* (Saunders, A. D. and Norry, M. J., eds.), Geological Society Special Publication **42**, 313–345.
- Sun, X.-M., Zhang, M.-S., Yang, B.-J., Zhu, D.-F. and Wan, C.-B. (2000) Geological and geophysical features and their structural evolution in the Songliao Basin and adjacent regions. *J. Changchun Univ. Sci. Techn.* **30** (Suppl.), 8–13 (in Chinese).

- Chinese with English abstract).
- Taylor, S. W. and McLennan, S. M. (1985) *The Continental Crust: Its Composition and Evolution*. Blackwell Scientific Publications, Oxford, 312 pp.
- Wang P.-J., Du, X.-D., Wang, J. and Wang, D.-P. (1996) Chronostratigraphy and Stratigraphic Classification of the Cretaceous of the Songliao Basin. *Geologica Sinica* (English edition), **9**(2), 207–217.
- Wang, P.-J., Wang, S.-X., Qu, Y.-B. and Ren, Y.-G. (1999) Volcanic events of the Cretaceous Songliao basin: a case study of Yingcheng Formation. *J. Changchun Univ. Sci. Techn.* **29** (Suppl.), 50–55 (in Chinese with English abstract)
- Wang, P.-J., Liu, W.-Z., Wang, S.-X. and Song, W.-H. (2002)  $^{40}\text{Ar}/^{39}\text{Ar}$  and K/Ar dating on the volcanic rocks in the Songliao basin, NE China: constraints on stratigraphy and basin dynamics. *Int. J. Earth Sci.* **91**, 331–340.
- Wang, Y.-J. and Fan, Z.-Y. (1997) Discovery of Permian radiolarians in ophiolite belt on northern side of Xilamulun river, Nei Menggu, and its geological significance. *Acta Palaeontologica Sinica*, **36**(1), 58–69.
- Wang, Z.-W., Yang, J.-L. and Gao, R.-Q. (1993) *Petroleum Geology of Daqing Oil Field*. Petroleum Industry Press, Beijing, 818 pp. (in Chinese).
- Wu, F.-Y., Sun, D.-Y., Li, H.-M. and Wang, X.-L. (2001) The nature of basement beneath the Songliao Basin in NE China: geochemical and isotopic constraints. *Phys. Chem. Earth* (part A), **26**, 793–803.
- Yang, B.-J., Liu, C., Jiao, X.-H., Tang, J.-R., Li, C.-L., Liu, G.-X. and Yang, P.-H. (1999) The geophysical characteristics of Songliao basin basement. *J. Changchun Univ. Sci. Techn.* **29** (Suppl.), 13–19 (in Chinese with English abstract).
- Zhang, M.-S., Sun, X.-M., Peng, X.-D. and Zhang, S.-M. (1999) Mesozoic tectonic stages of the Songliao Basin and adjacent regions. *J. Changchun Univ. Sci. Techn.* **29** (Suppl.), 20–24 (in Chinese with English abstract).
- Zhang, Y.-X., Sun, Y.-S., Zhang, X.-Z. and Yang, B.-J. (1998) *Geotraverse from Manzhouli to Suifenhe, China* (map & guidebook). Geology Press, Beijing.
- Zhao, H.-L., Deng, J.-F., Chen, F.-J., Hu, Q. and Zhao, S.-K. (1996) Characteristics and tectonics of the mid-Jurassic ophiolite in the Wandashan ranges of Heilongjiang province. *J. China Univ. Geosciences* **21**, 428–432 (in Chinese with English abstract).
- Zhao, H.-L., Deng, J.-F., Chen, F.-J., Hu, Q. and Zhao, S.-K. (1998) Petrology of the Mesozoic volcanic rocks and the basin formation in the northeast China. *J. Graduate School, China Univ. Geosci.* **12**, 57–61 (in Chinese with English abstract).
- Zhao, X.-X., Coe, R. S., Zhou, Y., Wu, H. R. and Wang, J. (1990) New paleomagnetic results from northern China: collision and suturing with Siberia and Kazakhstan. *Tectonophysics* **181**, 43–81.
- Zhu, Q.-W., Lu, F.-X., Xie, Y.-H. and Zheng, J.-P. (1997) Volcanic rocks assemblages in active belt of spreading type in continental margin: study on Mesozoic volcanic rocks around Songliao basin. *Acta Petrologica Sinica* **13**, 551–561 (in Chinese with English abstract).
- Zorin, Y. A. (1999) Geodynamics of the western part of the Monglia-Okhotsk collisional belt, Trans-Baikal region (Russia) and Mongolia. *Tectonophysics* **306**, 33–56.